ResearchGate

See discussions, stats, and author profiles for this publication at:
https://www.researchgate.net/publication/239535309

Thermal kaon production in relativistic heavy-ion collisions

Article *in* Nuclear Physics A · September 2005

DOI: 10.1016/j.nuclphysa.2005.05.002 · Source: arXiv

CITATIONS
11

READS
7

3 authors, including:

Henry Giacaman
Birzeit University

29 PUBLICATIONS **788** CITATIONS

SEE PROFILE

Available from: Henry Giacaman
Retrieved on: 11 August 2016

Available online at www.sciencedirect.com
SCIENCE DIRECT®
Nuclear Physics A 759 (2005) 201–226
NUCLEAR PHYSICS A

Thermal kaon production in relativistic heavy-ion collisions

I. Zakout [a,*], W. Greiner [a], H.R. Jaqaman [b]

[a] *Institut für Theoretische Physik, J.W. Goethe Universität, Robert-Mayer-Straße 8-10, Postfach 111932, D-60054 Frankfurt am Main, Germany*

[b] *Physics Department, Bethlehem University, P.O. Box 9 Bethlehem, Palestinian Authority*

Received 9 November 2004; received in revised form 21 April 2005; accepted 10 May 2005

Available online 13 June 2005

Abstract

We study kaon production in hot and dense hypernuclear matter with a conserved zero total strangeness and a conserved small negative isospin charge fraction in order to make our results relevant to relativistic heavy-ion collisions. The baryons and kaons are treated as MIT bags in the context of the modified quark–meson coupling model. They interact with each other via the scalar mesons σ, σ^* and the vector mesons ω, ϕ as well as the isovector meson ρ. We adopt realistic sets of hyperon–hyperon interactions based on several versions of the Nijmegen core potential models. Our results indicate that the hyperons as well as the kaons are produced abundantly when the temperature increases and approaches the critical temperature for the phase transition to a quark–gluon plasma. Moreover we find that the kaons are only produced thermally and we find no kaon condensation in the regime explored by relativistic heavy-ion collisions.
© 2005 Elsevier B.V. All rights reserved.

PACS: 21.65.+f; 21.80.+a

1. Introduction

The quark–meson coupling (QMC) model incorporates the quark–gluon degrees of freedom while respecting the established model based on the hadronic degrees of freedom in

* Corresponding author.
E-mail address: zakout@th.physik.uni-frankfurt.de (I. Zakout).

0375-9474/$ – see front matter © 2005 Elsevier B.V. All rights reserved.
doi:10.1016/j.nuclphysa.2005.05.002

nuclei. It describes nuclear matter as a collection of nonoverlapping MIT bags interacting through the self-consistent exchange of scalar σ, σ^* and vector mesons ω, ϕ as well as the isovector meson ρ in the mean field approximation with the mesonic fields directly coupled to the quarks [1]. In the so-called modified quark–meson coupling model (MQMC) [2–4], it has been suggested that including a medium-dependent bag parameter is essential for the success of relativistic nuclear phenomenology. The density dependence of the bag parameter is introduced by coupling it to the scalar mesonic field [2,4]. We have used the MQMC to study the properties of nuclear matter and quark deconfinement at finite temperature [5–7] and the phase transition from the hadronic phase to the quark–gluon plasma [7,8]. We have also studied the properties of neutron stars in the context of MQMC [9].

In the present work we shall extend the MQMC to study the production of strange hadrons, especially kaons, in relativistic heavy-ion collisions. Elucidating the properties of kaon production and kaon condensation is important to specify the tricritical point of the phase transition from a QGP phase to a hadronic phase. The competition between pion and kaon condensation in the framework of a microscopic model has been considered at zero and finite temperatures in the space of quark chemical potentials [10]. We consider a system of strange hadronic matter with conserved zero total strangeness and a conserved small negative isospin charge fraction in order to make our results relevant to heavy-ion collisions. We also investigate the possibility for the onset of kaon condensation in such a system.

In the mean field approximation, the scalar meson σ with mass 550 MeV is supposed to simulate the exchange of correlated pairs of pions and may represent a very broad resonance observed in $\pi\pi$ scattering, while the vector meson ω is identified with an actual meson having a mass of about 780 MeV. The σ scalar and ω vector mesonic fields couple the up and down flavors. Also the scalar $\sigma^*(s\bar{s})$ and vector $\phi(s\bar{s})$ mesonic fields are actual mesons with masses 975 and 1020 MeV, respectively. They are introduced to couple to the strange flavor quark. Similarly, the mesonic isovector field ρ, which is essential for isospin charged nuclear matter, is an actual meson with mass 770. It exchanges the nonstrange flavor quarks. We assume hadronic matter to consist of the members of the SU(3) baryon octet and the kaon doublet. The pions are not explicitly included in the calculation because the contribution of one-pion exchange vanishes in spin and isospin saturated nuclear matter and so their inclusion will not have any effect on the quantities of interest in the present work such as baryon or strangeness density. The pions contribute to the total energy density and to the pressure, for instance, but these quantities are not calculated in the present work. For the purpose of calculating these latter quantities, the pions can be included as an ideal gas. The baryon octet is comprised of $(p, n, \Lambda, \Sigma^+, \Sigma^0, \Sigma^-, \Xi^0, \Xi^-)$ baryons while the kaon doublet is comprised of (K^+, K^0) mesons. In heavy-ion collisions the total net strangeness of the system is conserved during the collision. If the quark–gluon plasma is produced during the collision the net strangeness for the hadronic phase may not be conserved but the total net strangeness for both the hadronic and quark–gluon phases will be conserved.

Various calculations and models predict that metastable strange systems with strangeness fractions of order one and charge neutrality might exist in the hadronic phase at densities between two and three times nuclear matter saturation density [11,12]. However, the predicted phenomenon of metastability of strange hadronic matter and the actual

values of the binding energy depend specifically on the partly unknown hyperon potentials assumed in dense matter [11–14]. Recently, unconstrained Relativistic Mean Field calculations of a charge–neutral strangeness-rich hadronic system have been carried out with two sets of hyperon–hyperon (or YY) potentials, the first set is determined from the Nijmegen hard-core potential Model D [15], and the second set corresponds to the potentials obtained in a recent SU(3) extension of the Nijmegen soft-core potential Model NSC97 [16–19]. The differences between these two sets are essentially attributable to the extremely attractive $\Sigma\Sigma$ and $\Xi\Xi$ interactions in the second set which allow for the possibility of deeply bound nuclear matter with hyperons [20].

In the present work, we shall study the production of kaons in neutral as well as weakly isospin strange hadronic matter at finite temperature. We shall adopt realistic phenomenological fitting parameters which are calculated from the potential models. The outline of the paper is as follows. In Section 2 we write the equation of state. Then in Section 3 we present the two different sets of fitting parameters for the YY potentials. In Section 4, we present and discuss our results. Finally, we summarize our conclusions in Section 5.

2. The equation of state

The quark field $\psi_q(\vec{r},t)$ inside a bag of radius R_i representing a baryon of species i satisfies the Dirac equation

$$\left[i\gamma^\mu\partial_\mu - m_q^0 + \left(g_{q\sigma}\sigma - g_{q\omega}\omega_\mu\gamma^\mu\right) + \left(g_{q\sigma^*}\sigma^* - g_{q\phi}\phi_\mu\gamma^\mu\right) - g_{q\rho}\frac{1}{2}\vec{\tau}\cdot\vec{\rho}_\mu\gamma^\mu\right] \times \psi_q(\vec{r},t) = 0, \tag{1}$$

where m_q^0 is the current mass of a quark of flavor q. The current quark masses are taken, for the up and down flavor quarks, to be $m_u = m_d = 0$ while for the strange flavor $m_s = 150$ MeV. Inclusion of small current quark masses for the nonstrange flavors or other values for the strange flavor leads only to small numerical refinements of the present results. In the mean field approximation the meson fields are treated classically and the space like components of the vector fields vanish for infinite systems due to rotational invariance. As a result we get $\omega_\mu\gamma^\mu = \langle\omega_0\rangle\gamma^0 = \omega\gamma^0$ and $\phi_\mu\gamma^\mu = \langle\phi_0\rangle\gamma^0 = \phi\gamma^0$ and $\vec{\tau}\cdot\vec{\rho}_\mu\gamma^\mu = \tau_3\langle\rho\rangle\gamma^0 = \tau_3\rho\gamma^0 = 2I_{3i}\rho\gamma^0$. The nonstrange (up and down) flavor quarks are coupled to the scalar $\sigma(550)$ and vector $\omega(780)$ and isovector $\rho(980)$ mesons while the strange flavor quarks are coupled to $\sigma^*(975)$ and $\phi(1020)$.

For a given value of the bag radius R_i and scalar fields σ and σ^*, the quark momentum x_{qi} is determined by the boundary condition of confinement which, for quarks of flavor q in a spherical bag, reduces to $j_0(x_{qi}) = \beta_{qi}\, j_1(x_{qi})$, where

$$\beta_{qi} = \sqrt{\frac{\Omega_{qi}(\sigma,\sigma^*) - R_i m_q^*}{\Omega_{qi}(\sigma,\sigma^*) + R_i m_q^*}}. \tag{2}$$

We have defined the effective quark mass inside the bag as

$$m_q^* = m_q^0 - g_{q\sigma}\sigma - g_{q\sigma^*}\sigma^*, \tag{3}$$

and the effective quark energy is given by

$$\Omega_{qi}(\sigma,\sigma^*)/R_i = \sqrt{(x_{qi}/R_i)^2 + m_q^{*2}}. \tag{4}$$

The bag energy is given by

$$E_{\text{bag}_i} = E_{\text{quarks}_i} - \frac{Z_i}{R_i} + \frac{4\pi}{3} R_i^3 B_i(\sigma,\sigma^*), \tag{5}$$

where

$$E_{\text{quarks}_i} = \sum_q^{n_q} \frac{\Omega_{qi}(\sigma,\sigma^*)}{R_i} \tag{6}$$

is the total constituent quarks kinetic energy inside the bag and $\frac{Z_i}{R_i}$ term is the zero-point energy of the quarks and $B_i(\sigma,\sigma^*)$ is the medium-dependent bag parameter.

We would like to emphasize here that we did not take into account the thermal excitation of the constituent quarks inside the bag [5–7,21]. In Refs. [5–7,21], the total constituent quarks kinetic energy with thermal excitations of the populated quarks is given by

$$E_{\text{quarks}_i} = \sum_q^{n_q} \frac{\Omega_{qi}(\sigma,\sigma^*)}{R_i} \big(f_q\big[\epsilon_q^* - \mu_q\big] - f_q\big[\bar{\epsilon}_q^* + \mu_q\big]\big), \tag{7}$$

where $f_q[\epsilon_q^* - \mu_q]$ and $f_q[\bar{\epsilon}_q^* + \mu_q]$ are the Fermi–Dirac quark and antiquark distribution functions, respectively. The constituent quark effective energy is given by

$$\epsilon_q^* = \frac{\Omega_{qi}(\sigma,\sigma^*)}{R_i} + \left(g_{q\omega}\omega + g_{q\phi}\phi + \frac{1}{2} g_{q\rho}\tau_3\rho\right) \tag{8}$$

and

$$\bar{\epsilon}_q^* = \frac{\Omega_{qi}(\sigma,\sigma^*)}{R_i} - \left(g_{q\omega}\omega + g_{q\phi}\phi + \frac{1}{2} g_{q\rho}\tau_3\rho\right). \tag{9}$$

In this construction, the constituent quark chemical potential μ_q is determined from the constraint

$$n_q = \sum_q^{n_q} f_q\big[\epsilon_q^* - \mu_q\big] - f_q\big[\bar{\epsilon}_q^* + \mu_q\big], \tag{10}$$

where n_q is the number of the constituent quarks (antiquarks) inside the bag. This constraint, fortunately, gives $f_q \approx 1$ and $\bar{f}_q \approx 0$ in the actual numerical calculations. We have found that adopting Eq. (6) rather Eq. (7) in the calculations does not affect the results given in Refs. [5–7]. Therefore, the thermal excitations of the populated quarks inside the bags in that construction is negligible [5–7].

In the simple QMC model, the bag parameter (constant) is taken as B_0 corresponding to its value for a free baryon. The medium effects are taken into account in the MQMC [2,3] by coupling the bag parameter to the scalar meson fields. In the present work we use the following generalized ansatz for the coupling of the bag parameter to the scalar fields σ and σ^* [7–9]:

$$B_i(\sigma,\sigma^*) = B_0 \exp\left[-4\left(g_{i\sigma}^{\text{bag}}\sigma + g_{i\sigma^*}^{\text{bag}}\sigma^*\right)/M_i\right] \tag{11}$$

with $g_{i\sigma}^{\text{bag}}$ and $g_{i\sigma^*}^{\text{bag}}$ as additional coupling constants to be fitted from the phenomenology. In Ref. [14], the bag parameter has been considered to couple to the nonstrange σ scalar field but not to the strange σ^* scalar field. The spurious center-of-mass energy is subtracted to obtain the effective baryon mass

$$M_i^* = \sqrt{E_{\text{bag}_i}^2 - \langle p_{\text{cm}}^2\rangle_i}, \tag{12}$$

where

$$\langle p_{\text{cm}}^2\rangle_i = \sum_q^{n_q} x_{qi}^2/R_i^2. \tag{13}$$

The bag radii R_i and R_k for baryon i and kaon k species, respectively, are obtained through the minimization of the baryon mass with respect to the bag radius [1]

$$\frac{\partial M_i^*}{\partial R_i} = 0. \tag{14}$$

The coupling of the scalar mean fields σ and σ^* with quarks in the nonoverlapping MIT bag through the solution of the point-like Dirac equation should be taken into account to satisfy the self-consistency condition. However, this constraint is essential to obtain the correct solution of the scalar mean field σ and σ^*. We think the discrepancy between our results in Ref. [5] and those in Ref. [21] is due to the coupling of the quark with the scalar mean fields σ, σ^* in the framework of the point like Dirac equation. The differentiation of the effective hadron species mass with respect to σ gives

$$\frac{\partial M_i^*}{\partial \sigma} = \frac{E_{\text{bag}_i}(\frac{\partial E_{\text{bag}_i}}{\partial \sigma})_{\sigma^*} - \frac{1}{2}(\frac{\partial \langle p_{\text{cm}}^2\rangle_i}{\partial \sigma})_{\sigma_*}}{M_i^*}, \tag{15}$$

where

$$\left(\frac{\partial E_{\text{bag}_i}}{\partial \sigma}\right)_{\sigma^*} = \sum_q \left(\frac{\partial E_{\text{bag}_i}}{\partial \Omega_{qi}}\right)\left(\frac{\partial \Omega_{qi}}{\partial \sigma}\right) + \left(\frac{\partial E_{\text{bag}_i}}{\partial \sigma}\right)_{\Omega_{qi}}, \tag{16}$$

$$\frac{\partial E_{\text{bag}_i}}{\partial \Omega_{qi}} = \sum_{q'} \frac{\delta_{q'q}}{R_i}, \tag{17}$$

and

$$\left(\frac{\partial E_{\text{bag}_i}}{\partial \sigma}\right)_{\Omega_{qi}} = \frac{4\pi}{3} R_i^3 \frac{\partial B_i(\sigma,\sigma^*)}{\partial \sigma}. \tag{18}$$

The $\frac{\partial \Omega_{qi}}{\partial \sigma}$ depends on x_{qi}. Its solution is obtained from the point-like Dirac equation for the quarks and must satisfy the required boundary condition as well as the confinement on the bag surface [1,2]. It reads

$$\frac{1}{R_i}\frac{\partial \Omega_{qi}}{\partial \sigma} = -g_{q\sigma}\langle \bar{\psi}_i|\psi_i\rangle, \tag{19}$$

where

$$\langle\bar{\psi}_i|\psi_i\rangle = \frac{\Omega_{qi}/2 + m_q^* R_i(\Omega_{qi} - 1)}{\Omega_{qi}(\Omega_{qi} - 1) + m_q^* R_i/2}. \tag{20}$$

Furthermore, the term for the spurious center-of-mass momentum correction reads

$$\frac{\partial\langle p_{\mathrm{cm}}^2\rangle_i}{\partial\sigma} = \frac{1}{R_i^2}\sum_q \frac{\partial x_{qi}^2}{\partial\sigma}, \tag{21}$$

where

$$\frac{\partial x_{qi}^2}{\partial\sigma} = \left(2\Omega_{qi}\frac{\partial\Omega_{qi}}{\partial\sigma}\right) + 2R_i^2 m_q^* g_{qi}. \tag{22}$$

Similar expressions can be obtained for the differentiation of the effective hadron (baryon and kaon) species mass with respect to the scalar mean field σ^*. The zero-point energy parameters Z_i of Eq. (4) are used to fit the actual masses of the free baryons $M_i = 939$, 1116, 1193 and 1315 MeV and are found to be $Z_i = 2.03$, 1.814, 1.629 and 1.505 for the N, Λ, Σ and Ξ hyperons respectively, corresponding to a free baryon bag parameter $B_0 = (188.1)^4$ MeV^4 and a free nucleon bag radius $R_0 = 0.6$ fm. The zero-point energy parameter Z_k is determined by fitting the actual mass of the free kaon $M_k = 495$ MeV which yields the value $Z_k = 1.170$.

The effective Fermi-energy for baryon and antibaryon species i is given by

$$\epsilon_i^*(p) = \sqrt{p^2 + M_i^{*2}} + X_i \tag{23}$$

and

$$\bar{\epsilon}_i^*(p) = \sqrt{p^2 + M_i^{*2}} - X_i, \tag{24}$$

respectively, where

$$X_i = [g_{i\omega}\omega + g_{i\phi}\phi + g_{i\rho}I_{3i}\rho]. \tag{25}$$

The effective Bose-energy for the kaon and antikaon species reads

$$\epsilon_k^*(p) = \sqrt{p^2 + M_k^{*2}} + X_k, \tag{26}$$

and

$$\bar{\epsilon}_k^*(p) = \sqrt{p^2 + M_k^{*2}} - X_k, \tag{27}$$

respectively, where

$$X_k = [g_{k\omega}\omega + g_{k\phi}\phi + g_{k\rho}I_{3k}\rho]. \tag{28}$$

The indices for the kaon and antikaon species are given by $k = (K^+, K^0)$ and $\bar{k} = (K^-, \bar{K}^0)$, respectively.

The chemical potentials μ_i and μ_k for baryon species i and kaon species k read

$$\mu_i = B_i\mu_B + S_i\mu_S + Q_i\mu_Q, \tag{29}$$

and

$$\mu_k = S_k \mu_S + Q_k \mu_Q, \tag{30}$$

respectively. The quantum numbers B_i, S_i and Q_i are the baryon, strangeness and isospin quantum numbers, respectively. The baryon, strangeness, isospin chemical potentials μ_B, μ_S and μ_Q, respectively, are determined from the constraints of total baryon, strange and isospin densities n_B Eq. (37), n_S^{Total} Eq. (38) and n_Q^{Total} Eq. (39), respectively.

The density for each baryon and antibaryon species is given by

$$n_i = \frac{d_i}{(2\pi)^3} \int d^3p\, f\big[\epsilon_i^*(p) - \mu_i\big], \tag{31}$$

and

$$\bar{n}_i = \frac{d_i}{(2\pi)^3} \int d^3p\, f\big[\bar{\epsilon}_i^*(p) + \mu_i\big], \tag{32}$$

respectively, where $d_i = 2$ is the spin degeneracy for the octet baryon species and f is the Fermi–Dirac distribution function

$$f[x] = \frac{1}{(e^{x/T} + 1)}. \tag{33}$$

Similarly, the density for each kaon and antikaon species is given by

$$n_k = \frac{d_k}{(2\pi)^3} \int d^3p\, b\big[\epsilon_k^*(p) - \mu_k\big], \tag{34}$$

and

$$\bar{n}_k = \frac{d_k}{(2\pi)^3} \int d^3p\, b\big[\bar{\epsilon}_k^*(p) + \mu_k\big], \tag{35}$$

respectively, where $d_k = 1$ is the kaon spin degeneracy, and b is the Bose–Einstein distribution function

$$b[x] = \frac{1}{(e^{x/T} - 1)}. \tag{36}$$

When the condition for kaon condensation (KC) [22,23] is not satisfied, see Eq. (52) below, the kaons will not condensate and the density of the kaon condensate $n_{\text{KC}} = 0$. In this case the chemical potentials μ_B, μ_S and μ_Q are determined from n_B, n_S^{Total} and n_Q^{Total}. However, when the condition for the kaon condensation $\mu_K = \epsilon_K^*(0)$ is satisfied for either kaon species K^+ or K^0 then that species will condensate. Beyond the condensation point, the strange chemical potential saturates at the threshold energy for the ground states $\mu_K \equiv \epsilon_K^*(0)$. On the other hand, if the condition $\mu_K = -\bar{\epsilon}_K^*(0)$ is satisfied for either K^- or $\bar{K}^0$ antikaon, then either K^- or $\bar{K}^0$ antikaon will condensate. Beyond the condensation point, the strange chemical potential saturates at the threshold energy for the ground states $\mu_K \equiv -\bar{\epsilon}_K^*(0)$. We shall return to the kaon condensation when we reach Eq. (52).

The baryon density reads,

$$n_B = \sum_i^{\text{Bs}} B_i [n_i - \bar{n}_i]. \tag{37}$$

The total strangeness density is given by

$$n_S = n_S^{\mathrm{Bs}} + n_S^{\mathrm{Ks}}, \tag{38}$$

where $n_S^{\mathrm{Bs}} = \sum_i^{\mathrm{Bs}} S_i[n_i - \bar{n}_i]$ and $n_S^{\mathrm{Ks}} = \sum_k^{\mathrm{Ks}} S_k[n_k - \bar{n}_k] + S_K n_{\mathrm{KC}}$. The total isospin density is given by

$$n_Q = n_Q^{\mathrm{Bs}} + n_Q^{\mathrm{Ks}}, \tag{39}$$

where $n_Q^{\mathrm{Bs}} = \sum_i^{\mathrm{Bs}} Q_i[n_i - \bar{n}_i]$ and $n_Q^{\mathrm{Ks}} = \sum_k^{\mathrm{Ks}} Q_k[n_k - \bar{n}_k] + Q_K n_{\mathrm{KC}}$.

The vector mean fields ω, ϕ and ρ are determined, respectively, as follows

$$\omega = \sum_i^{\mathrm{Bs}} \frac{g_{i\omega}}{m_\omega^2}[n_i - \bar{n}_i] + \sum_k^{\mathrm{Ks}} \frac{g_{k\omega}}{m_\omega^2}[n_k - \bar{n}_k] + \frac{g_{K\omega}}{m_\omega^2} n_{\mathrm{KC}}, \tag{40}$$

$$\phi = \sum_i^{\mathrm{Bs}} \frac{g_{i\phi}}{m_\phi^2}[n_i - \bar{n}_i] + \sum_k^{\mathrm{Ks}} \frac{g_{k\phi}}{m_\omega^2}[n_k - \bar{n}_k] + \frac{g_{K\phi}}{m_\phi^2} n_{\mathrm{KC}}, \tag{41}$$

$$\rho = \sum_i^{\mathrm{Bs}} \frac{g_{i\rho}}{m_\rho^2} I_{3i}[n_i - \bar{n}_i] + \sum_k^{\mathrm{Ks}} \frac{g_{k\rho}}{m_\rho^2} I_{3k}[n_k - \bar{n}_k] + \frac{g_{K\rho}}{m_\rho^2} I_{3k} n_{\mathrm{KC}}. \tag{42}$$

The $g_{i\omega}$, $g_{i\phi}$ and $g_{i\rho}$ are the meson–baryon coupling constants while $g_{k\omega}$, $g_{k\phi}$ and $g_{k\rho}$ are the meson–kaon coupling constants and are determined from the data.

The pressure for hot and dense strange nuclear matter is equal to the negative of the grand thermodynamic potential density and is given by

$$\begin{aligned} P = {} & \frac{1}{3}\sum_i^{\mathrm{Bs}} \frac{d_i}{(2\pi)^3} \int d^3p \frac{p^2}{\epsilon_i^*}\big(f\big[\epsilon_i^*(p) - \mu_i\big] + f\big[\bar{\epsilon}_i^*(p) + \mu_i\big]\big) + P_K \\ & + \frac{1}{2}m_\omega^2\omega^2 + \frac{1}{2}m_\phi^2\phi^2 + \frac{1}{2}m_\rho^2\rho^2 - \frac{1}{2}m_\sigma^2\sigma^2 - \frac{1}{2}m_{\sigma^*}^2\sigma^{*2}, \end{aligned} \tag{43}$$

where summation i runs over the 8 species of the baryon octet p, n, Λ, Σ^+, Σ^0, Σ^- and Ξ^0, Ξ^-. The thermal kaon pressure is given by

$$P_K = \frac{1}{3}\sum_k^{\mathrm{Ks}} \frac{d_k}{(2\pi)^3} \int d^3k \frac{k^2}{\sqrt{k^2 + M_k^{*2}}}\big(b\big[\epsilon_k^*(k) - \mu_k\big] + b\big[\bar{\epsilon}_k^*(k) + \mu_k\big]\big), \tag{44}$$

where the summation k run over the kaon doublet species K^+, K^0.

The scalar mean fields σ and σ^* are calculated by maximizing the pressure

$$\frac{\partial P}{\partial \sigma} = 0, \tag{45}$$

$$\frac{\partial P}{\partial \sigma^*} = 0. \tag{46}$$

The pressure depends explicitly on the scalar mean fields σ, σ^* through the last two terms in Eq. (43). It also depends on the baryon and kaon effective masses M_i^* and M_k^* which in turn depend on σ and σ^*. If we write the pressure as a function of $(\{M_i^*\}, \{M_k^*\})$ and

(σ, σ^*), the extremization of $P(\{M_i^*\}, \{M_k^*\}, \sigma, \sigma^*)$ with respect to the scalar fields σ and σ^* can be written as

$$\frac{\partial P}{\partial \sigma} = \sum_i \left(\frac{\partial P}{\partial M_i^*}\right)_{\{M_j\}_{j\neq i}, \mu_B, \mu_S \mu_Q, T} \frac{\partial M_i^*}{\partial \sigma} + \left(\frac{\partial P}{\partial \sigma}\right)_{\{M_j\}} = 0. \tag{47}$$

A similar expression can be written for $\frac{\partial P}{\partial \sigma^*} = 0$. The coupling of the scalar mean fields σ, σ^* with the quarks in the nonoverlapping MIT bags through the solution of the point-like Dirac equation should be taken into account to satisfy the self-consistency condition. This constraint is essential to obtain the correct solution of the scalar mean field σ, σ^*.

The pressure of the kaon condensate P_{KC}, if it exists, contributes to the total pressure of hot and dense strange hadronic matter. The total pressure of the system becomes

$$P^{\mathrm{total}} = P + P_{\mathrm{KC}}. \tag{48}$$

The contribution of the kaon condensate pressure reads [24,25]

$$P_{\mathrm{KC}} = \frac{1}{2}(f\theta)^2\big[\epsilon_k^*(0) - \mu_k\big]\big[\bar{\epsilon}_k^*(0) + \mu_k\big], \tag{49}$$

where

$$\epsilon_k^*(0) = M_k^* + X_k, \tag{50}$$

$$\bar{\epsilon}_k^*(0) = M_k^* - X_k. \tag{51}$$

This equation is derived by assuming that the kaon amplitude is replaced by the ansatz $K = f\theta/\sqrt{2}$ and $K\bar{K} = \frac{1}{2}f^2\theta^2$ where f is the kaon decay constant and θ is the dimensionless kaon field strength. The variation of Eq. (49) gives

$$\delta P_{\mathrm{KC}} = f^2\theta\big[\epsilon_k^*(0) - \mu_k\big]\big[\bar{\epsilon}_k^*(0) + \mu_k\big] = 0. \tag{52}$$

There are three solutions to Eq. (52) that determine the conditions for kaon condensation. The trivial solution is that kaon amplitude vanishes $\theta = 0$. This case means that no kaon condensation takes place in the system and subsequently $n_{\mathrm{KC}} = 0$. The other two solutions are determined as follows: if $[\epsilon_k^*(0) - \mu_k] = 0$ either $k = (K^+$ or $K^0)$ will condensate, and if $[\bar{\epsilon}_k^*(0) + \mu_k] = 0$ either antikaon $k = (K^-$ or $\bar{K}^0)$ will condensate. The density of the kaon condensate is given by,

$$n_{\mathrm{KC}} = (f\theta)^2(\mu_k - X_k). \tag{53}$$

In this case, the charge chemical potential becomes $\mu_Q(\epsilon_K^*(0), \mu_S)$ for either K^+or K^0 condensate or $\mu_Q(-\bar{\epsilon}_K^*(0), \mu_S)$ for either K^- or $\bar{K}^0$ condensate since $\mu_K = S_K\mu_S + Q_K\mu_Q$ and n_S^{Total} is conserved. It is interesting to note here that the three solutions give $P_{\mathrm{KC}} = 0$ and normally the pressure of the condensate kaons contributes indirectly via the strange hadronic abundances and the total energy density of the system.

3. Fitting parameters for *YY* potentials

We assume that the σ and ω mesons couple only to the up and down quarks while σ^* and ϕ couple to the strange quark. We thus set $g_{r\phi} = g_{r\sigma^*} = g_{s\sigma} = g_{s\omega} = 0$ and $g_{s\rho} = 0$, where

r refers to the up and down flavors while s denotes the strange flavor. By assuming the SU(6) symmetry of the simple quark model we have the relations $g_{s\sigma^*} = \sqrt{2}g_{r\sigma}$ and $g_{s\phi} = -\sqrt{2}g_{r\omega}$. The σ mean field is supposed to simulate the exchange of correlated pairs of pions and may represent a very broad resonance observed in $\pi\pi$ scattering. We take $m_\sigma = 550$ MeV. The vector ω and ρ mesons are identified with the actual mesons whose masses are $m_\omega = 783$ MeV and $m_\rho = 770$ MeV, respectively. Since the mean fields, σ and ω, are considered as $\langle u\bar{d}\rangle$ condensates, they interact only with u, d-quark in the baryons and kaons. On the other hand, the scalar and vector mean fields σ^*, ϕ are considered as $\langle s\bar{s}\rangle$ condensates and interact only with the s-quarks in the baryons and kaons. The isovector mean fields interact with the u, d-quarks in the baryons and kaons.

The coupling of each baryon species with the vector mesons is calculated by counting the constituent quarks

$$g_{i\omega} = \sum_q^3 g_{q\omega} = \sum_r g_{r\omega}, \tag{54}$$

and

$$g_{i\phi} = \sum_q^3 g_{q\phi} = \sum_s g_{s\phi}, \tag{55}$$

while

$$g_{i\rho} = g_{q\rho}. \tag{56}$$

With these assumptions the only free parameters left at our disposal are the quark–meson coupling constants $g_{r\sigma}$ and $g_{r\omega}$ and the bag coupling constants $g_{i\sigma}^{\text{bag}}$, $g_{i\sigma^*}^{\text{bag}}$ for the 4 baryon species and these parameters are adjusted to fit nuclear properties as well as the extrapolated properties of hypernuclear matter. The coupling constants of the scalar and vector mesons to the nonstrange quarks are taken as $g_{r\sigma} = 1$ and $g_{r\omega} = 2.705$ which together with a bag coupling constant $g_{N\sigma}^{\text{bag}} = 6.81$ yield a binding energy of 16 MeV and a compressibility K_V^{-1} of 289 MeV at the normal saturation density $\rho_0 = 0.17$ fm^{-3} of nuclear matter [2,5,6]. The isospin vector meson coupling constant for the ρ-meson is taken as $g_{q\rho} = 8.086$ to reproduce the bulk symmetry energy. The coupling constants $g_{i\sigma}^{\text{bag}}$ and $g_{i\sigma^*}^{\text{bag}}$, where $i = \Lambda, \Sigma, \Xi$ are determined from the YY potentials assumptions.

In the present calculation, we have considered two different models for the hyperon–hyperon interactions. Table 1 summarizes the values of the two sets of coupling constants corresponding to these two models. The basic quark–meson coupling constants as well as the parameters $g_{i\sigma}^{\text{bag}}$ are identical in the two models and are chosen to fit nuclear and hypernuclear properties. In particular, the parameters $g_{i\sigma}^{\text{bag}}$ are determined by fitting the hyperon potentials in nuclear matter [12]:

$$\begin{aligned} U_\Lambda^{(N)}(\rho_0) &= -30 \text{ MeV}, \\ U_\Sigma^{(N)}(\rho_0) &= +30 \text{ MeV}, \\ U_\Xi^{(N)}(\rho_0) &= -18 \text{ MeV}, \end{aligned} \tag{57}$$

Table 1
Fitting parameters

Fit set	$g_{q\sigma}$	$g_{q\omega}$	$g_{q\rho}$	$g^{\text{bag}}_{N\sigma}$	$g^{\text{bag}}_{\Lambda\sigma}$	$g^{\text{bag}}_{\Lambda\sigma^*}$	$g^{\text{bag}}_{\Sigma\sigma}$	$g^{\text{bag}}_{\Sigma\sigma^*}$	$g^{\text{bag}}_{\Xi\sigma}$	$g^{\text{bag}}_{\Xi\sigma^*}$	$g^{\text{bag}}_{K\sigma}$	$g^{\text{bag}}_{K\sigma^*}$	$g_{K\omega}$
Model Ia	1.0	2.705	8.086	6.81	4.22	5.45	1.63	7.26	2.27	9.12	2.27	$\sqrt{2}\times 2.27$	$g_{q\omega}$
Model Ib	1.0	2.705	8.086	6.81	4.22	5.45	1.63	7.26	2.27	9.12	2.27	$\sqrt{2}\times 2.27$	$1.7g_{q\omega}$
Model II	1.0	2.705	8.086	6.81	4.22	0.0	1.63	10.28	2.27	10.17	2.27	$\sqrt{2}\times 2.27$	$g_{q\omega}$

where the hyperon potentials are defined by

$$U_i^{(i)} = \left(M_i^* - M_i\right) + (g_{i\omega}\omega + g_{i\phi}\phi). \tag{58}$$

However, the two models differ in their choices for the constants $g^{\text{bag}}_{i\sigma^*}$.

Model I is designed to mimic the consequences of the Nijmegen hard-core potential Model D [12,13,15]. It is nevertheless constrained by Λ and Ξ nuclear phenomenology, and by a few $\Lambda\Lambda$ hypernuclei reported to date. It accounts more realistically for the attractive $\Lambda\Lambda$ and $N\Xi$ interactions, but ignores the Σ hyperons altogether. In this model, the medium constants $g^{\text{bag}}_{i\sigma^*}$ are adjusted so that the potential of a single hyperon embedded in a bath of Ξ matter becomes

$$U_\Xi^\Xi(\rho_0) = U_\Lambda^\Xi(\rho_0) = -40 \text{ MeV} \tag{59}$$

in accordance with the attractive hyperon–hyperon interaction of the Nijmegen hard core potential Model D [12,14]. Furthermore, we adopt the approximation $U_\Xi^\Xi(\rho_0) \approx U_\Sigma^\Xi(\rho_0)$ to fit the medium constants. The resulting $U_\Lambda^{(\Lambda)}(\rho_0/2)$ is about -20 MeV.

Model II is designed to generate qualitatively similar baryon potentials to those obtained in the BHF approximation from the SU(3) extensions of the Nijmegen soft-core potential model NSC97 [16–19]. The phenomenology in this model departs substantially from that in Model I. The NSC97 model has been tuned up to reproduce certain characteristics of Λ hypernuclei, particularly its version NSC97f. It yields particularly attractive $\Xi\Xi$, $\Sigma\Sigma$ and $\Sigma\Xi$ interactions. Some of the shortcomings of this model are the vanishingly weak $\Lambda\Lambda$ and $N\Xi$ interactions which are in contradiction with the little experimental evidence available from $\Lambda\Lambda$ hypernuclei and from Ξ-nucleus interaction. In this model we adjust the bag constants $g^{\text{bag}}_{i\sigma^*}$ to reproduce qualitatively the binding energy curve of each hyperon species in its own hyperonic matter B_i^i as those produced by the Model NSC97f [18,20]. No binding occurs for Λ hyperons while Σ matter is deeply bound at -33 MeV per baryon at ρ_{Σ_0} which is twice as deep as ordinary nuclear matter, and Ξ matter has an energy of -23 MeV per baryon at ρ_{Ξ_0}.

The kaon coupling constants are determined from the kaon potentials when embedded in nuclear matter $U_{K^+}^{(N)} = 20$ MeV [26] and $U_{K^-}^{(N)} = -120$ to -180 MeV [24,25,27]. In Model I, we have used two slightly different versions of these coupling constants. In set (Ia) we have taken $g_{K\omega} = g_{q\omega}$ based on simple SU(6) symmetry while in set (Ib) we have taken $g_{K\omega} = 1.7g_{q\omega}$ in order to fit the kaon potential depths [26]. In both sets we take $g^{\text{bag}}_{K\sigma} = 2.27$ and $g^{\text{bag}}_{K\sigma^*} = \sqrt{2}g^{\text{bag}}_{K\sigma}$. In Model II, we only take $g_{K\omega} = g_{q\omega}$ based on simple SU(6) symmetry. In our calculations we shall adopt $g_{K\omega} = g_{q\omega}$ as the normal case and we shall consider the case $g_{K\omega} = 1.7g_{q\omega}$ as a special case. Here it may be worth mentioning

that recent results [28] indicate that $U_{K^-}^{(N)} = -50$ to -60 MeV and for such a shallow kaon potential the renormalization factor need not be as large as 1.7.

4. Results and discussions

We have studied hadronic matter with a conserved strangeness density $n_S = 0$ at finite temperature using the MQMC model which takes into account the quark degrees of freedom as well as the medium dependence of the bag constant B. We have chosen a direct coupling of the bag parameter B to the scalar mean fields σ and σ^* and the bag parameter becomes $B \equiv B(\sigma, \sigma^*)$. The quarks and antiquarks confined in the bags are coupled to the scalar mean fields σ and σ^* and the vector mean fields ω and ϕ and isovector mean field ρ. At first, we have studied the symmetric hot and dense strange hadronic system of baryons and kaons with a neutral isospin charge $n_Q/n_B = 0$ and with a conserved zero net strangeness $n_S = 0$. Then, we have considered the asymmetric system with a conserved isospin charge n_Q/n_B and a conserved zero net strangeness. This is relevant for heavy-ion collisions where it is possible to have an asymmetric system with a conserved low isospin fraction in the range $n_Q/n_B = 0.0$ to -0.2.

The starting point of the calculation is the determination of the chemical potentials μ_B, μ_S and μ_Q using the baryon, strange and isospin densities given by Eqs. (37), (38) and (39), respectively. The vector mean-fields ω and ϕ and the isovector mean field ρ are computed from Eqs. (40), (41) and (42), respectively. Once the values for the chemical potentials (μ_B, μ_S, μ_Q) are given, the values for the scalar mean fields σ and σ^* are calculated by maximizing the pressure using Eqs. (45) and (46), respectively. These constraints should take into account the coupling of the quark with the scalar mean fields in the frame of the point-like Dirac equation exactly [1–3] to obtain consistent results. The bag radius for each hadron species is obtained by minimizing the hadron mass with respect to its bag radius, Eq. (14).

In Fig. 1, we display the density fraction for each baryon species $x_i = (n_i - \bar{n}_i)/n_B$ versus the baryonic density n_B at several temperatures using the parameter sets (Ia) and (Ib). Furthermore we also display in the lower part of panel (a) of this figure the relative abundance of the kaons. The abundance of the strange hadrons up to $T = 50$ MeV is completely negligible and this explains why the 5 MeV curve cannot be distinguished from the horizontal axes of the panels (b), (c) and (d). The strange hadrons make their first noticeable appearance at $T \approx 80$ MeV and they start to be produced abundantly when the temperature exceeds 100 MeV. The Σ appears to be produced more abundantly than the Λ only because it has a higher isospin degeneracy factor. On the other hand, the Ξ has the lowest rate of production. The dependence of the production rates of the various hadronic species on the total baryon density seems to undergo a drastic change at the critical temperature $T_c = 170$ MeV of the QGP phase transition, becoming almost flat above this temperature. We also note that the modification of the kaon vector coupling which leads to the two sets (Ia) and (Ib) has very little effect on the production of the various hadronic species. The effect can be mainly seen above T_c where set (Ia) produces slightly more Ξ and, to a lesser extent, more Σ and kaons than set (Ib) because of the stronger vector coupling for kaons in (Ib). Kaon production in the system increases with temperature especially for tempera-

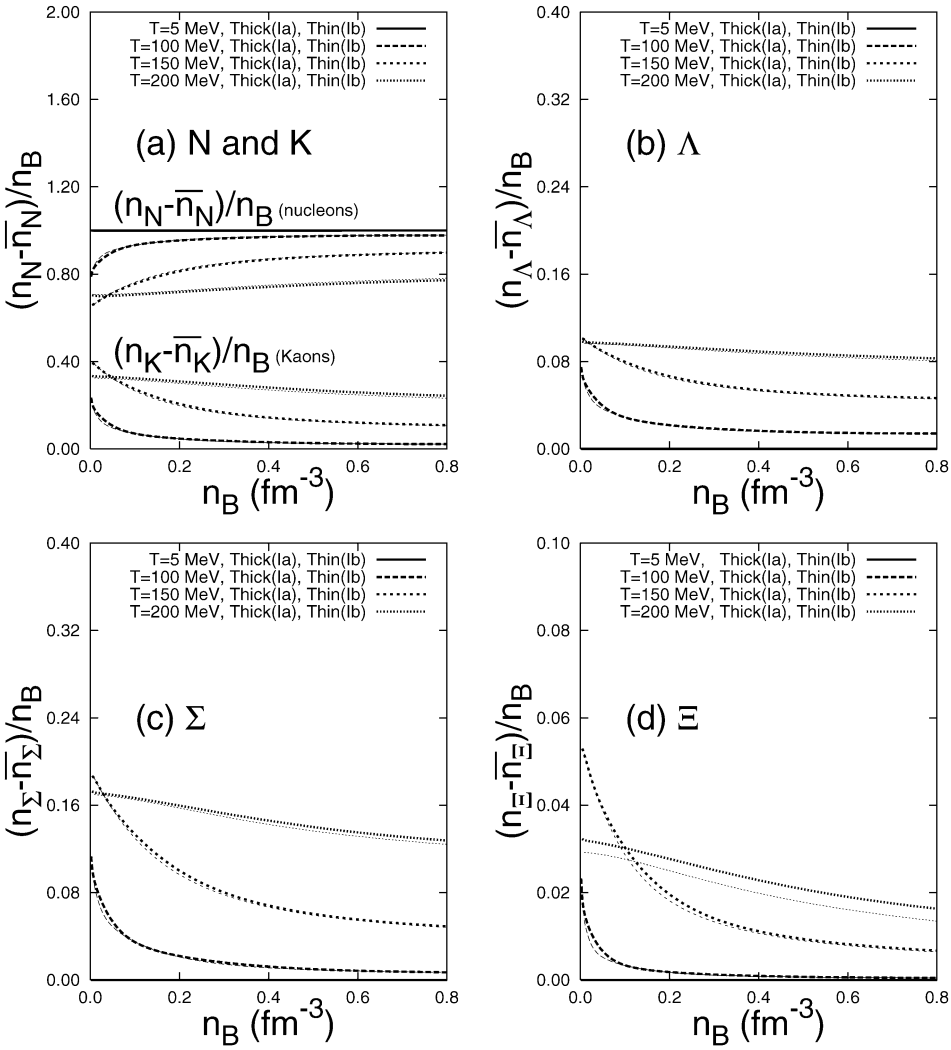

Fig. 1. The density fraction for hadron and antihadron species $x_i = (n_i - \bar{n}_i)/n_B$ versus baryonic density n_B at several temperatures using the parameter sets (Ia) and (Ib). (a) Nucleons and kaons, (b) Λ, (c) Σ, (d) Ξ.

tures exceeding $T \approx 100$ MeV. We see that a large mesonic strangeness $n_S^K > 0.2$ can be reached at the critical temperature $T_c = 170$ MeV when kaons are produced abundantly in the system.

In Fig. 2, we compare the baryon and kaon abundances obtained using parameter sets (Ia) and (II). The phenomenology in model (II) departs substantially from that in (Ia) for large baryonic and strangeness densities where the phase transition to $\Sigma\Sigma$ takes place [8,20]. We see that at high temperatures the Λ is more abundantly produced with the set (Ia) than when the set (II) is used. The Σ has the opposite behavior, as its abundance obtained from the set (Ia) is less than that from the set (II). At the same time, there is no

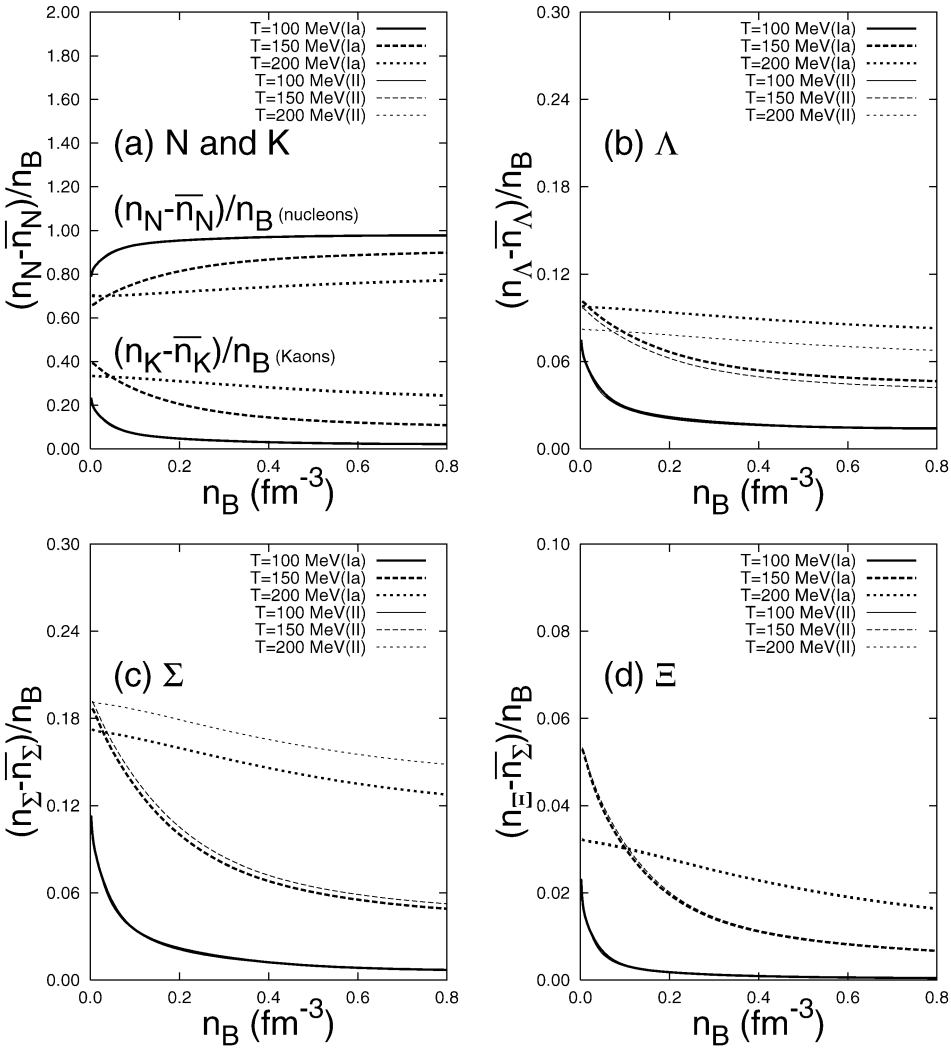

Fig. 2. Same as Fig. 1 but using parameter sets (Ia) and (II).

noticeable difference between the two models in the nucleon, kaon and cascade production rates. Furthermore, there is not much difference in total strange baryon production. Generally speaking, it can be concluded that kaon production and condensation in the context of MQMC is not likely to be affected drastically by which set is being used from amongst the different sets of parameters extracted from phenomenology.

In Fig. 3, we display the antibaryon to baryon abundance ratio for each baryon species $\bar{n}_i/n_i$ at several temperatures as obtained by using parameter set (Ia). It is seen that for temperatures $T < 100$ MeV the production of the antibaryons is negligible. However, for higher temperatures there is significant antibaryon production particularly when the tem-

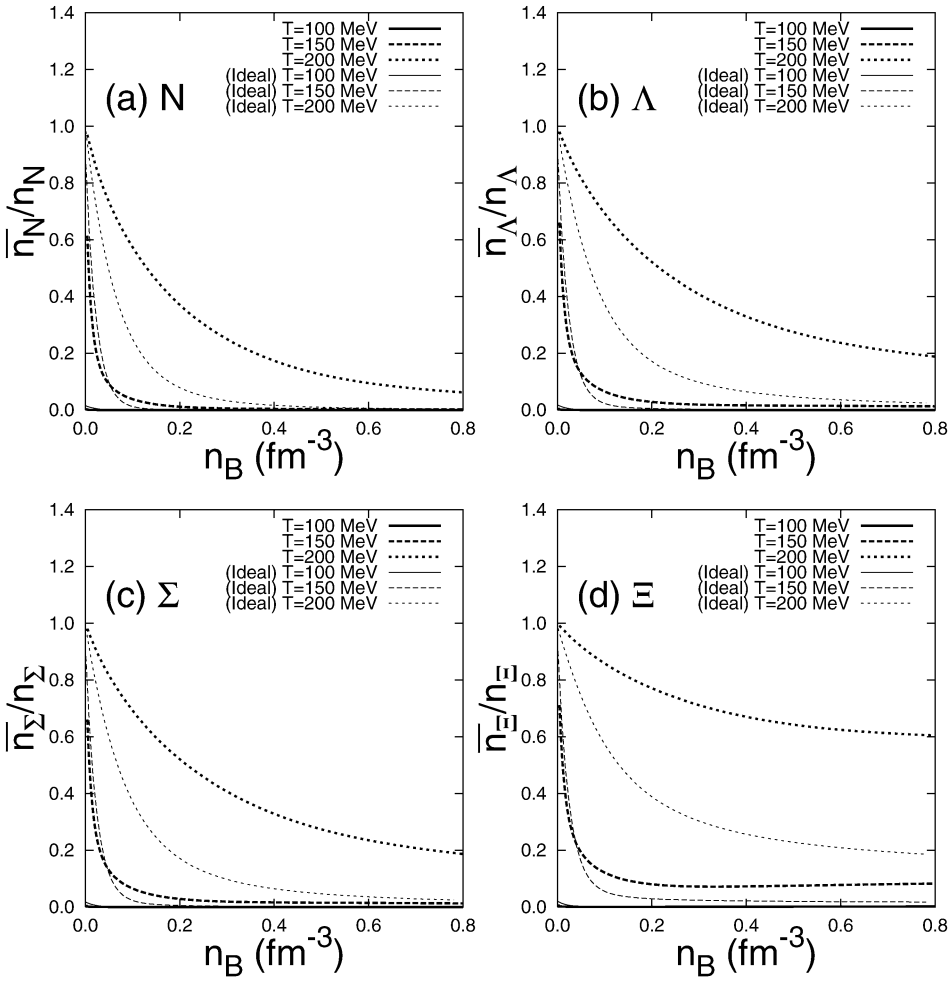

Fig. 3. The ratio of antibaryon to baryon abundance $\bar{n}_i/n_i$ for each baryon species versus baryonic density n_B at several temperatures using the parameter set (Ia) and for the ideal gas approximation. (a) N, (b) Λ, (c) Σ, (d) Ξ.

perature reaches and exceeds T_c. Furthermore, we notice that the antibaryon abundance ratio $\bar{n}_i/n_i$, is particularly large at small baryon density n_B. This ratio also seems to increase with the baryon strangeness number as follows:

$$\frac{\bar{\Xi}}{\Xi} > \frac{\bar{\Lambda}}{\Lambda}, \frac{\bar{\Sigma}}{\Sigma} > \frac{\bar{N}}{N}. \tag{60}$$

This enhancement of antihyperon abundance ratio over the antiproton abundance ratio in the relativistic nuclear collisions has been observed earlier [29]. Also included in Fig. 3 are the results obtained in the ideal gas approximation which assumes noninteracting hadrons in a thermal bath. In this approximation, the hadrons do not modify their masses, do not interact with each other and there are no mean fields at all. Although this approximation

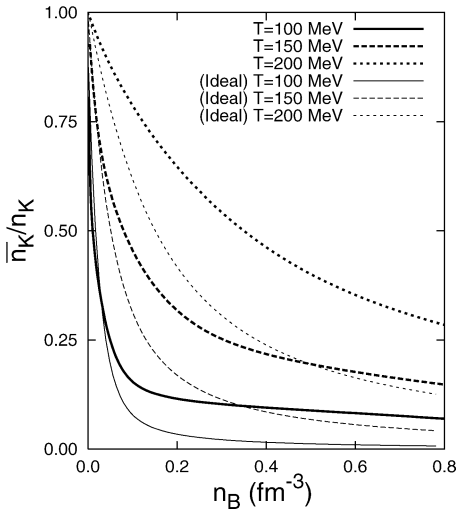

Fig. 4. The ratio of antikaon to kaon abundance $\bar{n}_K/n_K$ at various temperatures using the parameter set (Ia) and for the ideal gas approximation.

is too simplistic, it can be useful to obtain rough first estimates. It is seen from Fig. 3 that the ideal gas results greatly underestimate the antibaryon production, especially at high temperature or at high density. In Fig. 4, we show the antikaon to kaon abundance ratio versus the baryon density n_B at various temperatures using parameter set (Ia) and in the ideal gas approximation. We note that the antikaon abundance ratio increases with temperature. We also note that again the ideal gas approximation gives much lower estimates for the antikaon to kaon abundance ratio than the MQMC, especially at high temperature or at high density.

Fig. 5 examines the crucial issue of the onset of kaon condensation in heavy-ion collisions. Kaon condensation implies that the equation of state will be softer and that more hyperons and kaons will accumulate in the system. Indeed, it is known that kaon condensation plays a significant role in the physics of neutron stars [27]. One of the major themes of the present work is to study the possibility for the onset of kaon condensation in heavy-ion collisions. The necessary condition for the onset of kaon condensation is to nontrivially satisfy Eq. (52). For the K^0 or K^+ kaons, condensation is possible only when

$$\mu_k = \epsilon_k^*(0) \tag{61}$$

while for the antikaons $\bar{K}^0$ or K^-, condensation is possible only when

$$\mu_k = -\bar{\epsilon}_k^*(0). \tag{62}$$

When the condition for the onset of kaon condensation is satisfied, the kaons start to condense smoothly and the strange chemical potential could be evaluated either from Eq. (61) or (62). After the kaon condensation starts to take place in the system, the strange chemical potential μ_S becomes an input parameter and the amplitude of the kaon condensation is calculated by conserving the total strangeness of the system. The contribution of the

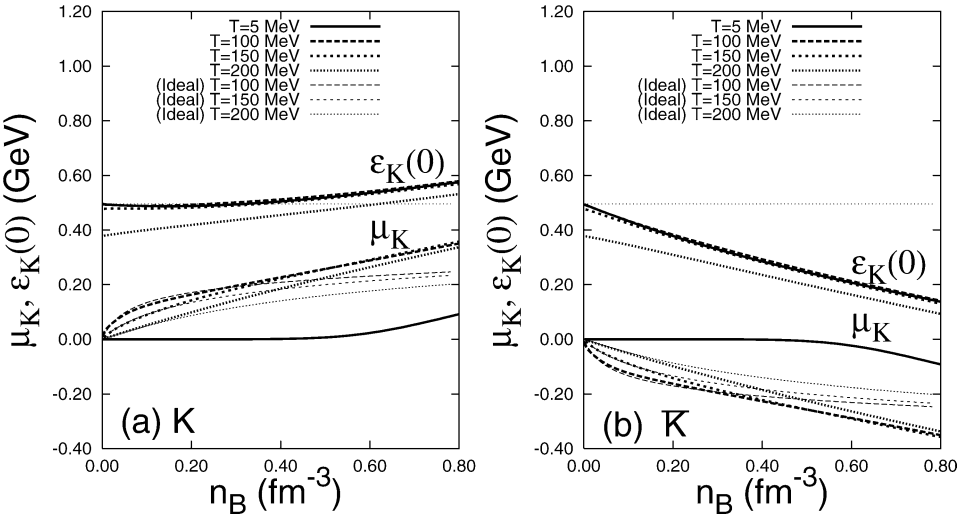

Fig. 5. The strange chemical potential μ_S and the kaon threshold effective energy $\epsilon_k^*(0)$ versus baryonic density n_B for various temperatures using the parameter set (Ia). (a) Kaons, (b) antikaons.

kaon condensate to the total density of the system is calculated from Eq. (53). To examine the possibility for the onset of kaon condensation in our model we plot in Fig. 5 the kaon chemical potential μ_K and the kaon threshold effective energy $\epsilon_k^*(0)$ versus the baryonic density n_B at various temperatures. The isospin chemical potential μ_Q vanishes for symmetric strange hadronic matter so that in this case Eq. (30) reduces to $\mu_K = \mu_S$, where μ_S is the strangeness chemical potential. We see from panel (a) of Fig. 5 that the kaon chemical potential μ_K is always less than the kaon threshold energy $\epsilon_k^*(0)$ for the all baryon densities n_B so that Eq. (61) can never be satisfied. A similar conclusion can be drawn for the antikaons and Eq. (62) as can be seen from panel (b) of the same figure. This indicates that kaon condensation does not take place at any temperature and density in heavy-ion collisions where the total strangeness is conserved to zero for a system that consists of baryons and kaons. The kaons are only produced thermally in this system. The situation is, of course, completely different in neutron stars where there is enough time for the conservation of strangeness to be violated by the weak interaction [27].

In Figs. 6 and 7, we display the baryon and kaon effective masses versus the baryon density n_B. We note that, in the context of the MQMC model, the effective masses do not vanish at large baryon densities, unlike the standard Walecka model where the effective hadronic masses tend to vanish at large baryon density. The realistic case of effectively massive hadrons at all densities is actually a characteristic result of the MQMC. Indeed, in the hadronic phase, the hadron's effective mass should not vanish until chiral symmetry is restored or a QGP phase transition takes place. At the phase transition, there is a sharp drop in the hadron's effective masses and all hadrons in the system will dissolve into their constituent quarks. Furthermore, the quarks attain their current masses which are very small for the up and down flavors. At this point, however, bubbles of the QGP are formed in the system. Therefore, we do not find it is appropriate, in the realistic situation relevant to

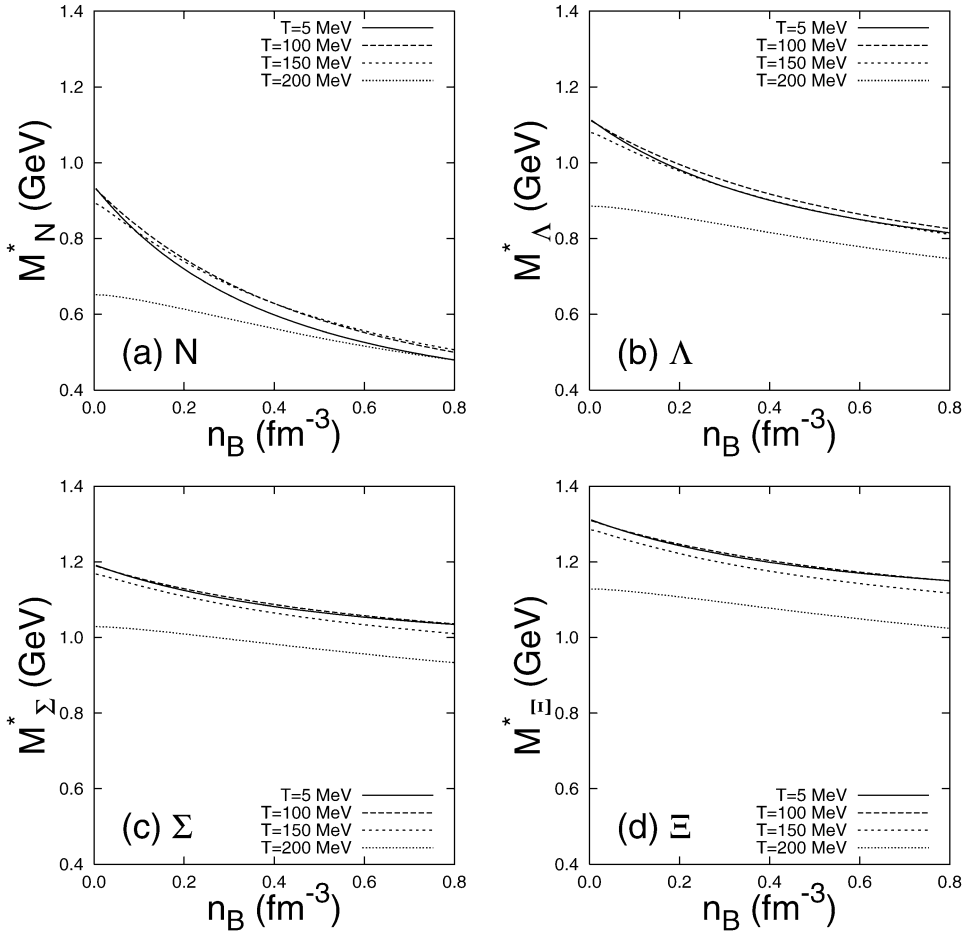

Fig. 6. The effective mass M_i^* for each baryon species versus baryonic density n_B for various temperatures using the parameter set (Ia). (a) N, (b) Λ, (c) Σ, (d) Ξ.

heavy-ion collisions, to extrapolate the study of the onset of kaon condensation to massless hadrons since these massless hadrons can exist only at the point of the phase transition.

We have also extended MQMC to study hot and dense asymmetric strange hadronic matter with a conserved total zero strangeness $n_S/n_B = 0$ and a conserved finite negative isospin density fraction $n_Q/n_B \leqslant 0$. Generally speaking, the negative value of the isospin density fraction n_Q/n_B reflects the fact that the number of neutrons is more than the number of protons (i.e. $n_n > n_p$) in the initial conditions of the colliding heavy ions. The results for the asymmetric system are therefore more relevant to relativistic heavy-ion collisions. We present our results for such a system using the parameter set (Ia) in Figs. 8 and 9 for $n_Q/n_B = -0.10$, while the results for $n_Q/n_B = -0.20$ are shown in Figs. 10 and 11.

In Figs. 8 and 10, we display the net kaon abundance ratio $x_K = (n_K - \bar{n}_K)/n_B$ and the ratio of antikaon abundance over kaon abundance for the charged and neutral kaon species (K^+, K^0) at several temperatures for the isospin charge density fractions $n_Q/n_B = -0.1$

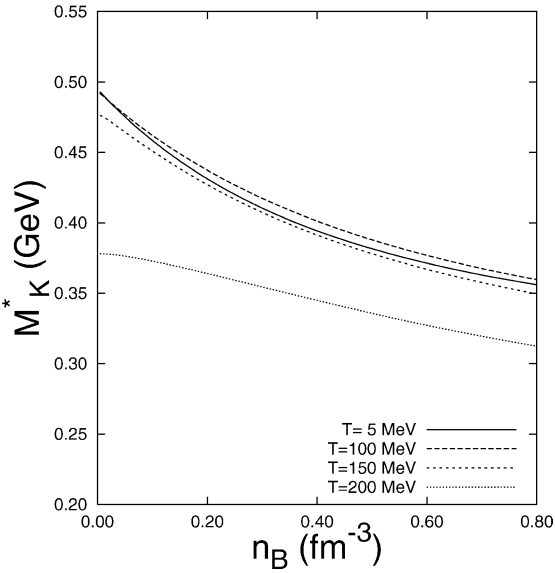

Fig. 7. The effective kaon mass M_K^* versus baryonic density n_B for various temperatures using the parameter set (Ia).

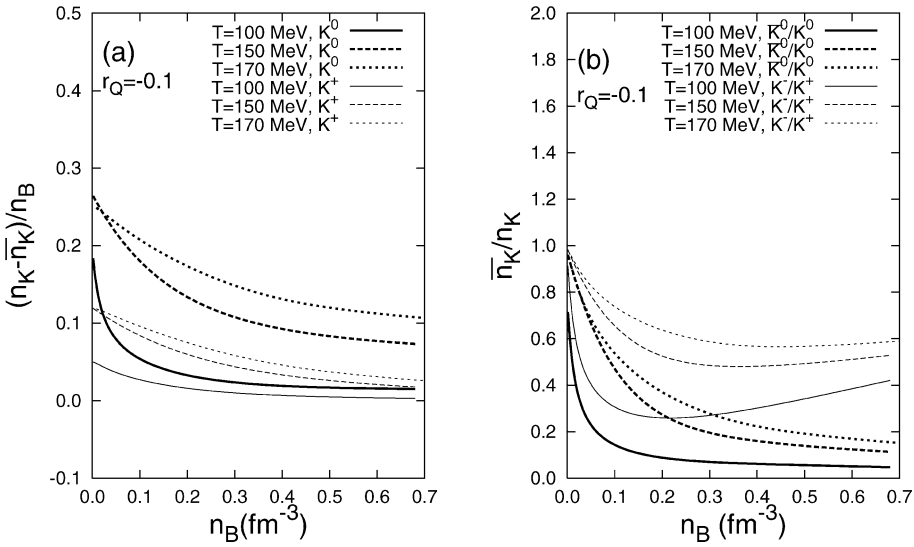

Fig. 8. The kaon abundance versus baryonic density n_B for various temperatures for $n_Q/n_B = -0.1$ using the parameter set (Ia). (a) The kaon density fraction $x_K = (n_K - \bar{n}_K)/n_B$, (b) the ratio of antikaon abundance over kaon abundance $\bar{n}_K/n_K$.

and $n_Q/n_B = -0.2$, respectively. In panel (a) of both figures, we display the net kaon abundance versus the baryon density n_B. It is seen that $x_{K^0} = (n_{K^0} - n_{\bar{K}^0})/n_B$ is much larger than $x_{K^+} = (n_{K^+} - n_{K^-})/n_B$ in such a system, especially at higher temperatures.

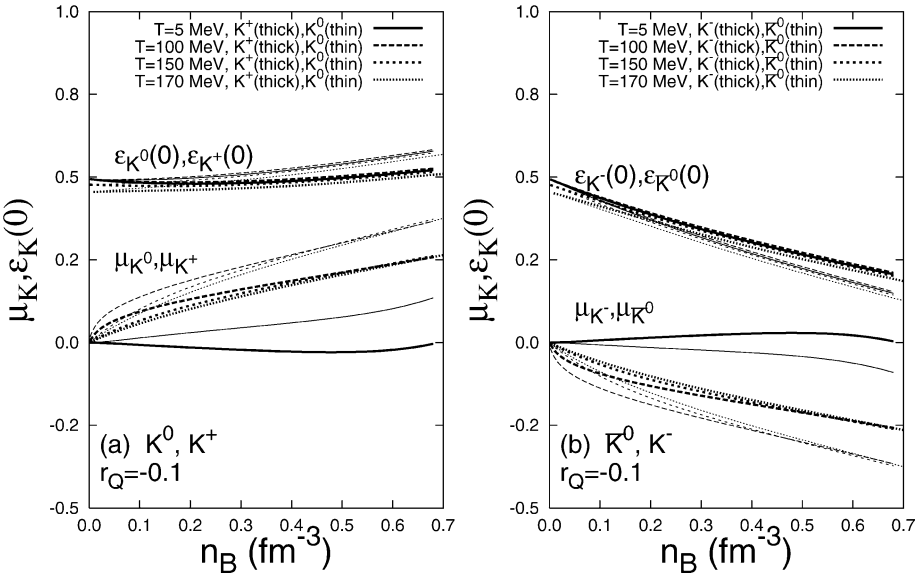

Fig. 9. The strange chemical potential μ_S and the kaon threshold effective energy $\epsilon_k^*(0)$ versus baryonic density n_B at various temperatures for $n_Q/n_B = -0.1$ using the parameter set (Ia). (a) Kaons, (b) antikaons.

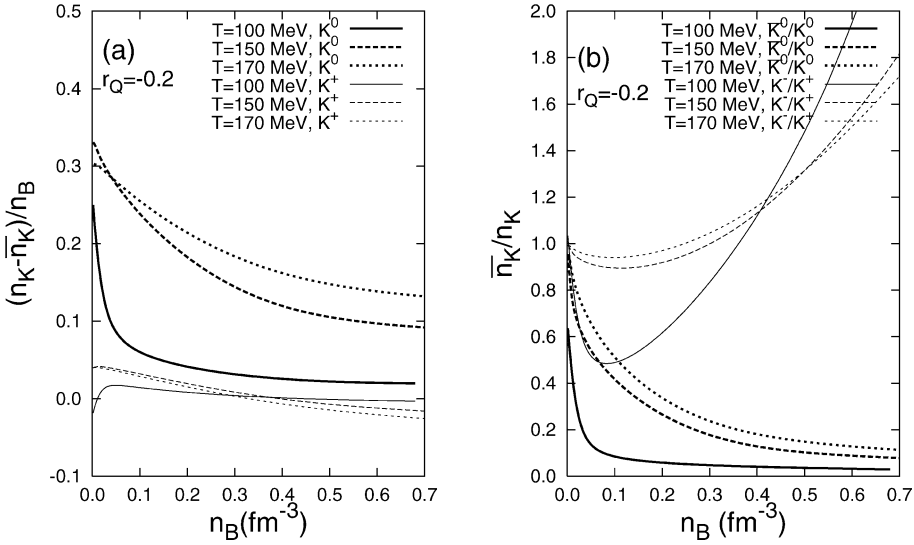

Fig. 10. Same as Fig. 8 but with $n_Q/n_B = -0.2$.

The conservation of net strangeness for the asymmetric system is more easily preserved by neutral kaons at high temperatures. Consequently, when the negative isospin n_Q/n_B is increased, the neutral kaons become more dominant than the charged ones. From Fig. 8(b), we see that the K^0 and K^+ are produced more abundantly than their antiparticles for the

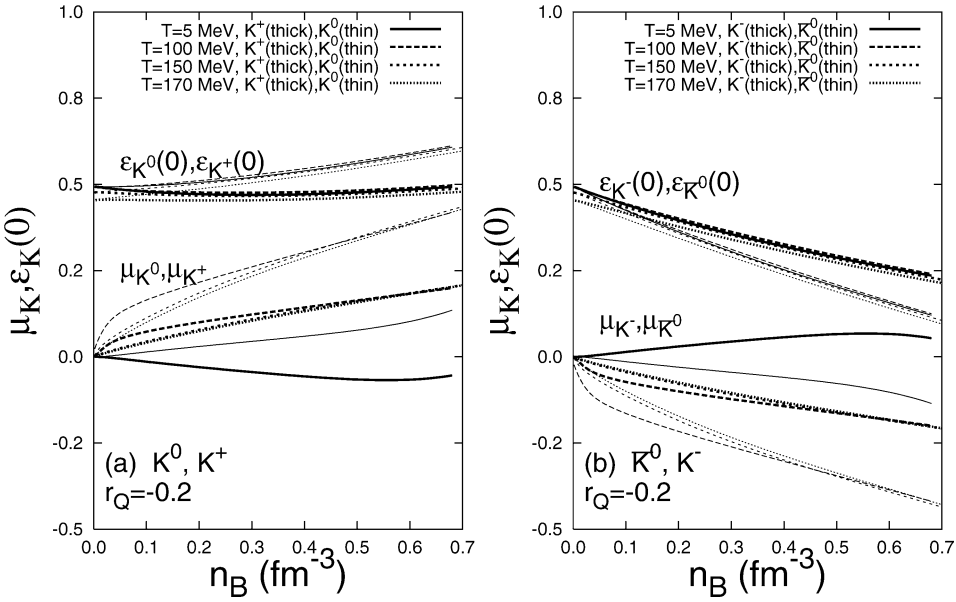

Fig. 11. Same as Fig. 9 but with $n_Q/n_B = -0.2$.

system with lower asymmetry. However, when the asymmetry is increased, we see from Fig. 10(b) a dramatic change for the charged kaons with the antiparticle K^- becoming more abundant than the K^+ at high densities in order to conserve isospin. Actually, in addition to the kaons, we have found that the baryon species Σ^-, Σ^0, Σ^+ also play an important role in conserving the isospin n_Q/n_B at high temperature when the isospin charge fraction is increased. The proton density fraction tends to saturate at some value when the negative isospin charge fraction becomes rather large ($n_Q/n_B = -0.2, n_p/n_B \approx 0.30$) while the density fraction for neutrons continues to increase with temperature. However, at higher temperatures, the conservation of isospin charge fraction is preserved by creating more charged strange hadrons.

We have also examined the possibility for the onset of kaon condensation in the asymmetric system. The necessary condition for kaon condensation is that the kaon threshold energy $\epsilon_k^*(0)$ equal its chemical potential μ_K. In Figs. 9 and 11, we display the kaon chemical potential μ_K and the kaon threshold effective energy $\epsilon_k^*(0)$ versus the baryonic density n_B at various temperatures and for $n_Q/n_B = -0.1$ and $n_Q/n_B = -0.2$, respectively. We see that the kaon's threshold energy is always larger than its chemical potential, and their curves become almost parallel at large baryonic density. Furthermore, when the nuclear matter asymmetry is increased by increasing the negative isospin n_Q/n_B to reach the maximal value of $n_Q/n_B = -0.5$, appropriate for neutron matter, the onset of kaon condensation is not possible even at very large baryonic densities and we find that the strange chemical potential μ_S in the medium is always modified in such a manner as to avoid the onset of kaon condensation. These results show that no signature can be expected for kaon condensation in heavy-ion collisions and kaons can only be produced thermally.

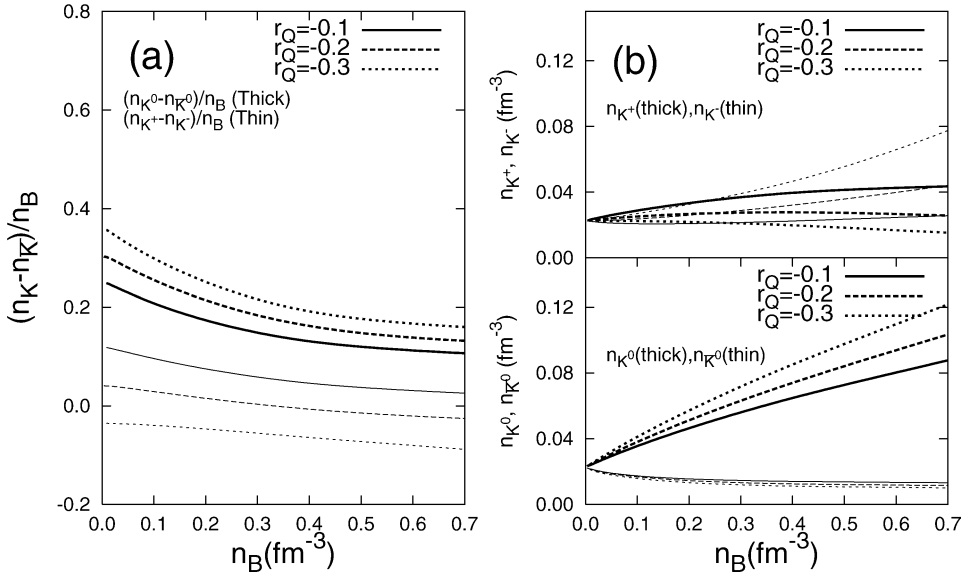

Fig. 12. The kaon and antikaon abundances versus baryonic density n_B for various isospin charge ratios n_Q/n_B at temperature $T = 170$ MeV using the parameter set (Ia). (a) The density fraction $x_K = (n_K - n_{\bar{K}})/n_B$ for the charged and neutral kaons, (b) the kaon and antikaon abundances for charged (upper panel) and neutral (lower panel) kaons.

We have also examined how the production of the charged and neutral kaons and their antiparticles at high temperature varies with respect to the isospin charge ratio n_Q/n_B. In Fig. 12, we display the kaon and antikaon abundances versus the baryonic density n_B at temperature $T = 170$ MeV for $n_Q/n_B = -0.1, -0.2, -0.3$. The temperature $T = 170$ MeV is particularly interesting because it is accessible at RHIC energies and is relevant to the freezeout chemical potential [30,31]. Part (a) of Fig. 12 displays the charged and neutral kaon abundant density fractions, x_K, while part (b) displays the densities for charged (upper panel) and neutral (lower panel) kaons and their antiparticles. It is seen from part (b) that the kaons and their antiparticles are produced abundantly at high temperatures even at very low baryon densities. However, the net density fraction for charged kaons $x_K = (n_{K^+} - n_{K^-})/n_B$ tends to be small and varies weakly with the baryon density n_B. Furthermore, it decreases when the asymmetry of the system increases by increasing the negative value of the isospin charge fraction n_Q/n_B. This reflects the fact that the negative charged kaons become more dominant as the magnitude of the isospin charge asymmetry increases and exceeds $|n_Q/n_B| = 0.25$. Here it must be stressed that in a realistic situation the isospin charge fraction of the normally used colliding heavy ions lies in the range $n_Q/n_B = 0$ to -0.1 and consequently K^+ production is expected to be more dominant than K^- in RHIC. However, more asymmetric nuclear matter may be reached experimentally in the future by using different isotopes for the colliding heavy ions. Generally speaking, the net production of charged kaons is relatively smaller than that of the neutral kaons, indicating that the neutral kaons play a more significant role in asymmetric nuclear matter in order to conserve the net zero strangeness of the system.

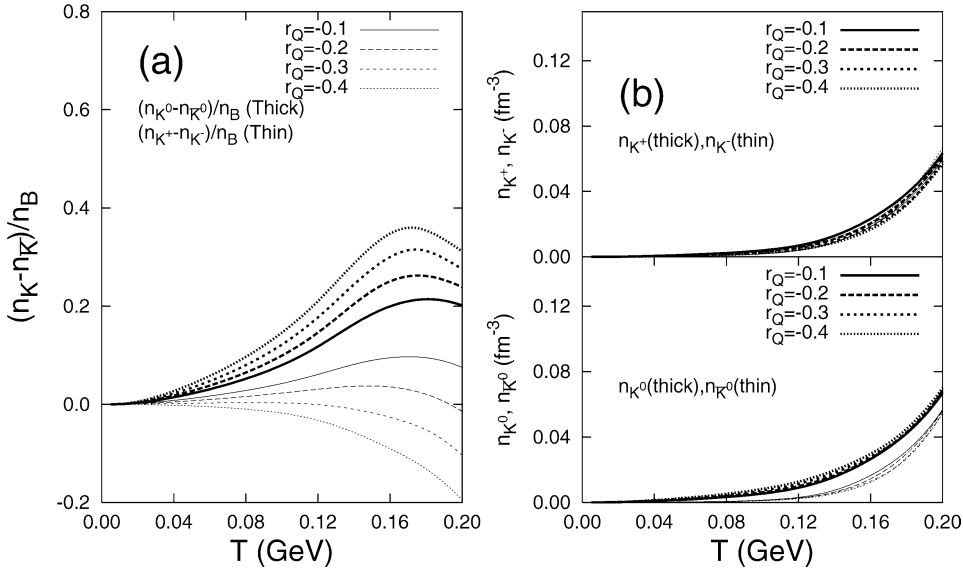

Fig. 13. Same as Fig. 12 but versus temperature at the baryonic density $n_B = 0.05$ fm^{-3}.

Fig. 13 displays the variation of kaon and antikaon abundances with respect to the temperature for several values of the isospin charge fraction n_Q/n_B. The calculations are carried out at the baryonic density $\rho_B = 0.05$ fm^{-3}. This rather small baryonic density is accessible in RHIC and has a special interest at high temperature in particular in studying the freezeout chemical potential [30,31]. The phase transition from the hadronic phase to QGP is expected to take place at this low baryon density and temperature $T = 170$ MeV. It is seen that kaons are produced abundantly when the temperature exceeds $T > 120$ MeV and this production becomes more significant when the temperature reaches $T = 170$ MeV. Furthermore, it is seen that the neutral kaon density, n_{K^0}, lies always above the antikaon density $n_{\bar{K}^0}$ but this is not the case for the charged kaons, n_{K^+} and n_{K^-}. The net density fraction for the charged kaons decreases as the magnitude of the negative isospin charge asymmetry increases while net density fraction for the neutral kaons has the opposite behavior. Moreover, the net density for the neutral kaons is always greater than that for the charged kaons for asymmetric nuclear matter. This reflects the fact that the K^0 abundance is dominant at all temperatures and more so as the magnitude of the isospin charge asymmetry increases.

In Fig. 14, we display the baryon, strangeness and isospin chemical potentials versus the baryonic density n_B at $T = 170$ MeV for the symmetrical and asymmetrical nuclear matter. We also indicate on this figure the estimated freezeout chemical potential at SPS and RHIC energies. In particular it is known that freezeout in RHIC occurs at the small chemical potential $\mu_B \approx 46 \pm 5$ MeV and at a temperature $T \approx 174 \pm 7$ MeV [30,31]. The substantial decrease of the baryon chemical potential from $\mu_B \approx 270$ MeV at SPS energies to $\mu_B \approx 45$ MeV at RHIC energies shows that, at mid-rapidity, we are dealing with a low net baryon density in the medium [30]. In our model, the baryon chemical

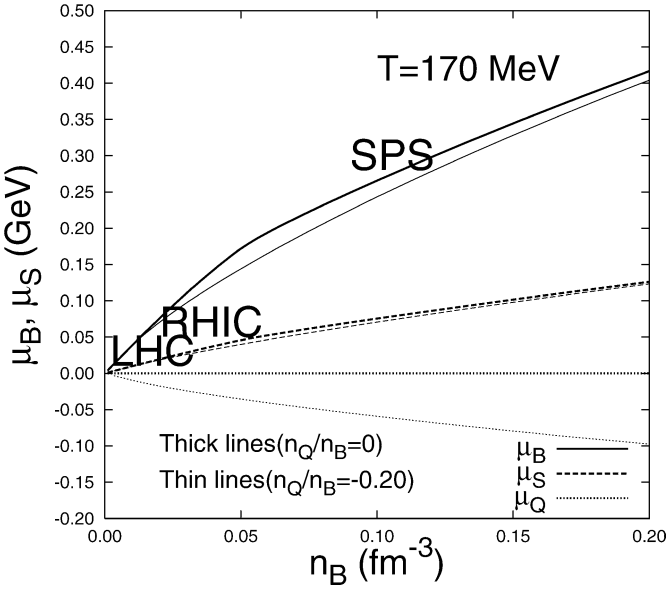

Fig. 14. The dependence of baryon, strange and isospin chemical potentials μ_B, μ_S and μ_Q, respectively, on the baryon density n_B at $T = 170$ MeV for a symmetric and an asymmetric matter.

potential $\mu_B \approx 50$ MeV for the critical temperature $T \approx 170$ MeV corresponds to the very small baryonic density $n_B \approx 0.015$ fm^{-3}. Other models, however, may lead to somewhat higher values for the baryonic density for the chemical freezeout potential [31] and we shall refer to a baryon density $n_B \approx 0.05$ fm^{-3} when we speak about RHIC physics.

5. Conclusions and summary

We have studied strange hadronic matter composed of the baryon octet and kaon doublet with a conserved zero total strangeness $n_S/n_B = (n_S^{\text{Baryons}} + n_S^{\text{Kaons}})/n_B = 0$ and a conserved finite isospin fraction n_Q/n_B. RHIC physics is reached at the rather low baryonic density $n_B \approx 0.05$ fm^{-3} and high temperature $T \approx 150$–170 MeV [30]. We have not found any evidence for kaon condensation even in highly asymmetric dense nuclear matter. The kaon threshold energy is always higher than the kaon chemical potential given by Eq. (30) so that the kaons are only produced thermally in the system. The production of the strange hadrons starts smoothly at low temperatures and then they are abundantly produced when the temperature reaches $T \approx 170$ MeV.

We have solved the baryon, strange and isospin chemical potentials μ_B, μ_S and μ_Q, respectively, self-consistently. In the hot or even warm dense medium, the strange chemical potential μ_S is finite (nonzero) even for a system with zero total strangeness and it likely modifies itself in a manner to decrease the kaon chemical potential to be always lower than the kaon threshold energy. The results of other microscopic models also disfavor kaon with respect to pion condensation [10]. On the other hand, in cold dense matter, the strange

chemical potential μ_S is normally set to zero for a system with zero total strangeness. In this case, it is possible for the antikaon (kaon) to condense at zero temperature at very high baryonic density. Therefore, the results at finite temperature suggest that μ_S must be actually assigned a small finite value at zero temperature in order to maintain the conservation of the zero total strangeness for cold dense matter. Such a modification would also reduce the possibility for the onset of kaon condensation at $T = 0$.

It is interesting to note here that the effective hadronic masses do not vanish in the hadronic phase in our model. The effective hadronic masses attain small values only at the chiral phase transition and the phase transition to the QGP. In the QGP, the hadrons dissolve and disappear and the kaons will not be produced. On the other hand, at very high densities and low temperatures the quark color superconductivity will dominate. The strange hadrons and their antiparticles are normally produced at high temperatures and low baryonic densities which are the ideal circumstances at RHIC energies. Furthermore, when the system freezes out, the strange baryons and kaons might survive with the baryonic sector having a negative net strangeness $n_S^{\text{baryons}}/n_B = 0.0$ to -0.25 and the mesonic sector (i.e. kaons) having a positive net strangeness, but the total strangeness for the baryons and kaons is conserved to zero. Moreover, although K^0 production always dominates over $\bar{K}^0$, the K^- becomes more abundant than K^+ for highly asymmetric nuclear matter (i.e. $n_Q/n_B < -0.2$), especially at high temperatures or large baryonic densities.

Acknowledgements

I.Z. gratefully acknowledges support from the Alexander von Humboldt Foundation. The authors are indebted to the Deutsche Forschungsgemeinschaft for financial support during the early stages of the present project through the grant GR 243/51-1. I.Z. and H.R.J. thank G. Shahin for his assistance in the computational work. I.Z. thanks C. Greiner, J. Schaffner-Bielich, L. Tolos and J.-P. Leroy for interesting discussions and comments.

References

[1] K. Saito, A.W. Thomas, Phys. Lett. B 327 (1994) 9.
[2] X. Jin, B.K. Jennings, Phys. Rev. C 54 (1996) 1427.
[3] X. Jin, B.K. Jennings, Phys. Lett. B 374 (1996) 13.
[4] H. Mueller, B.K. Jennings, Nucl. Phys. A 626 (1997) 966.
[5] I. Zakout, H.R. Jaqaman, Phys. Rev. C 59 (1999) 962.
[6] I. Zakout, H.R. Jaqaman, Phys. Rev. C 59 (1999) 968.
[7] I. Zakout, H.R. Jaqaman, S. Pal, H. Stöcker, W. Greiner, Phys. Rev. C 61 (2000) 055208.
[8] I. Zakout, H.R. Jaqaman, W. Greiner, J. Phys. G 27 (2001) 1939.
[9] S. Pal, M. Hanauske, I. Zakout, H. Stöcker, W. Greiner, Phys. Rev. C 60 (1999) 015802.
[10] A. Barducci, R. Casalbuoni, G. Pettini, L. Ravagli, hep-ph/0410250.
[11] J. Schaffner, C.B. Dover, A. Gal, C. Greiner, H. Stöcker, Phys. Rev. Lett. 71 (1993) 1328.
[12] J. Schaffner, C.B. Dover, A. Gal, C.G.D.J. Millener, H. Stöcker, Ann. Phys. 235 (1994) 35.
[13] S. Balberg, A. Gal, J. Schaffner, Prog. Theor. Phys. Suppl. 117 (1994) 325.
[14] P. Wang, R.K. Su, H.Q. Song, L. Zhang, Nucl. Phys. A 653 (1999) 166.
[15] M. Nagels, T. Rijken, J. de Swart, Phys. Rev. D 15 (1977) 2547.

[16] T.A. Rijken, V.G.J. Stoks, Y. Yamamoto, Phys. Rev. C 59 (1999) 2140.
[17] V.G.J. Stoks, T.A. Rijken, Phys. Rev. C 59 (1999) 3009.
[18] V.G.J. Stoks, T.-S.H. Lee, Phys. Rev. C 60 (1999) 024006.
[19] I. Vidana, A. Polls, A. Ramos, M. Hjorth-Jensen, V.G.J. Stoks, Phys. Rev. C 61 (2000) 025802.
[20] J. Schaffner-Bielich, A. Gal, Phys. Rev. C 62 (2000) 034311.
[21] P.K. Panda, A. Mishra, J.M. Eisenberg, W. Greiner, Phys. Rev. C 56 (1997) 3134.
[22] D.B. Kaplan, A.E. Nelson, Phys. Lett. B 175 (1986) 57.
[23] A.E. Nelson, D.B. Kaplan, Phys. Lett. B 192 (1987) 193.
[24] N.K. Glendenning, J. Schaffner-Bielich, Phys. Rev. Lett. 81 (1998) 4564.
[25] N.K. Glendenning, J. Schaffner-Bielich, Phys. Rev. C 60 (1999) 025803.
[26] K. Tsushima, K. Saito, A.W. Thomas, S.V. Wright, Phys. Lett. B 429 (1998) 239.
[27] V. Thorsson, M. Prakash, J.M. Lattimer, Nucl. Phys. A 572 (1994) 693.
[28] L. Tolos, A. Polls, A. Ramos, J. Schaffner-Bielich, Phys. Rev. C 68 (2003) 024903.
[29] J. Schaffner, I.N. Mishustin, L.M. Satarov, H. Stocker, W. Greiner, Z. Phys. A 341 (1991) 47.
[30] P. Braun-Munzinger, D. Magestro, K. Redlich, J. Stachel, Phys. Lett. B 518 (2001) 41.
[31] D. Zschiesche, S. Schramm, J. Schaffner-Bielich, H. Stöcker, W. Greiner, Phys. Lett. B 547 (2002) 7.